kept sufficiently low during compression that equilibrium transformations are blocked kinetically.

9. Q. Williams, E. Knittle, R. Reichlin, S. Martin, and R. Jeanloz [*J. Geophys. Res.* **95**, 21549 (1990)] and G. Richard and P. Richet [*Geophys. Res. Lett.* **17**, 2093 (1990)] demonstrated through a combination of x-ray diffraction, mid-infrared absorption spectroscopy, and transmission electron microscopy (TEM) that crystalline fayalite is transformed to a glass and not just crushed to a microcrystalline aggregate, upon room-temperature compression to pressures above 35 to 40 GPa. The TEM study demonstrated that amorphization was complete down to ~1 nm.
10. Samples were compressed at room temperature and to pressures >40 to 45 GPa with a gasketed Mao-Bell type diamond cell (*9*). In order to avoid contamination of the samples, no pressure medium was used. Also, different samples were prepared both with and without ruby being present for pressure calibration [see X. Li and R. Jeanloz, *Geophys. Res. Lett.* **14**, 1075 (1987)], but no difference was observed in our final results. Aliquots separated from our samples were examined by x-ray diffraction to determine that these were amorphized. We used the Debye-Scherrer method, with either filtered Cu K_α or monochromatized Mo K_α radiation, and mixed fine-grained Au with the sample to serve as an intensity standard [see M. B. Kruger and R. Jeanloz, *Science* **249**, 647 (1990); (*9*)]. By examining aliquots separated both before and after our magnetic measurements, we ensured that the samples were amorphous (that is, had not recrystallized) throughout the duration of our study.
11. F. A. Wedgwood and A. C. Wright, *J. Non-Cryst. Solids* **21**, 95 (1976).
12. The crystalline starting material is synthetic fayalite [H. Takei and S. Hosoya, in *High-Pressure Research in Geophysics*, S. Akimoto and M. H. Manghnani, Eds. (Center for Academic Publishing, Tokyo, 1982), p. 537] that has been used in numerous other studies (*9*). To verify our technique, the magnetic susceptibility of 94 (±2) μg of the crystalline sample, ground to a grain size of ~1 to 10 μm, was measured as a function of temperature. Measurements were then carried out on 34 (±5) μg of pressure-amorphized material, consisting of 18 samples that had been compressed in tungsten gaskets to over 40 GPa, and the results for the crystalline and pressure-amorphized materials are displayed in Fig. 1. All susceptibility measurements were made with a SHE superconducting quantum interference detector magnetometer operating over the temperature range 6 to 100 K. Susceptibility data were obtained at 1, 10, and 50 kOe for the polycrystalline sample, and at 20 and 30 kOe for the pressure-amorphized sample. The transition temperatures were unaffected by the different applied magnetic fields. The samples were loaded into a precalibrated container fabricated from an Al cylinder and lid, including a Kel-F (polychlorotrifluoroethylene) liner designed to minimize the contribution of the container to the measured moment of the sample. Thus, the resolution of our data is optimized by ensuring that the paramagnetism of the Al is nearly canceled by the diamagnetism of the Kel-F.
13. The structural and magnetic properties of crystalline fayalite are well known from a combination of x-ray diffraction, magnetic susceptibility, Mössbauer spectroscopy, and powder neutron diffraction measurements carried out as functions of temperature, the first three having been applied both to single-crystal and to polycrystalline samples (*14, 18*). The unit cell of fayalite is orthorhombic [*Pbnm*, *Z* (number of formula units per cell) = 4], containing eight Fe^{2+} ions distributed over two crystallographically distinct sites. These are the M1 (4a) sites (numbered 1 through 4) with only a center of symmetry and the M2 (4c) sites (numbered 5 through 8) with local symmetry including a mirror plane. Thus, the Néel transition at 65 (±2) K is found to be caused by collinear antiferromagnetic ordering (parallel to the *b* crystallographic axis) of the moments on the M2 sites, along with a canted antiferromagnetic ordering of the moments on the M1 sites. In contrast, the apparent transition of crystalline fayalite at ~23 K is thought to be caused by the large anisotropy of the magnetic susceptibility, rather than by a change in magnetic ordering; specifically, the temperature dependence of the magnetization parallel to the *c* crystallographic axis changes rapidly below ~20 to 25 K (*14*). Both the canted M1 ordering and the anisotropy of the susceptibility below 65 K are due to the M1-M2 exchange interaction ($J_{15} - 2J_{35} > 0$) competing with the M1 single-ion anisotropy within the crystal.
14. H. D. Megaw, *Crystal Structures* (Saunders, Philadelphia, 1973); H. Fuess, O. Ballet, W. Lottermoser, *Adv. Phys. Geochem.* **7**, 185 (1988).
15. Our values deviate slightly from those reported by R. P. Santoro, R. E. Newnham, and S. J. Nomura [*Phys. Chem. Solids* **27**, 655 (1966)] for crystalline powders of fayalite, $\mu_{eff} = 6.03\ \mu_B$ and $\theta = -126$ K, but the discrepancy is not significant and probably results from differences in preferred orientation of the samples in the two studies. For comparison, single-crystal measurements yield Weiss constants of $\theta = -107$ K for the *a* and *b* crystallographic directions and −66 K for the *c* direction of fayalite [J. M. D. Coey and S. Ghose, *Adv. Phys. Geochem.* **7**, 162 (1988)]. Also, because of the extremely small size of our specimens, our values of μ_{eff} and θ are subject to additional uncertainties due to errors in sample mass (for example, unaccounted sample loss during handling) and to the possible presence of minor impurities (*16*).
16. The dominant source of error for our absolute values of magnetic susceptibilities, and the resulting paramagnetic moments, arises from the sample mass. The smaller moment in the amorphous state most likely arises from the quenching of the orbital contribution to the moment, thus decreasing the moment from $\mu = g[J(J+1)]^{0.5} = 6.70\ \mu_B$ to $\mu = 2[S(S+1)]^{0.5} = 4.9$ in reasonable agreement with our result.
17. We synthesized polycrystalline fayalite enriched in ^{57}Fe, used as starting material for the Mössbauer studies, by heating the component oxides to 1173 K under controlled oxygen fugacity (Fe-FeO buffer) at 1.5 GPa pressure. This material was characterized by x-ray diffraction and Mössbauer spectroscopy, the results being in good agreement with previous work (*18*). Samples were then pressure-amorphized in gaskets made of Re and were examined by x-ray diffraction as described above (*10*).
18. See Coey and Ghose in (*15*); S. S. Hafner, J. Stanek, M. J. Stanek, *Phys. Chem. Solids* **51**, 203 (1990).
19. The paramagnetic ($T > T_N$) Mössbauer spectrum of crystalline Fe_2SiO_4 fayalite is characterized by two doublets, with isomer shifts (IS) relative to Fe, quadrupole splittings (QS), and line widths (LW) of: IS = 1.26 and 1.31 mm/s, QS = 3.09 and 3.06 mm/s, and LW = 0.33 and 0.33 mm/s at 71 K. We found that a singlet (IS = 1.22 mm/s, QS = 0, and LW = 0.84 mm/s) and two doublets (IS = 0.99 and 1.02 mm/s, QS = 1.73 and 2.95 mm/s, and LW = 0.84 and 0.84 mm/s) yield a good fit to our paramagnetic spectra of the amorphous phase.
20. J. J. Hauser, *Phys. Rev. B* **22**, 2554 (1980).
21. H. P. Klug and L. E. Alexander, *X-Ray Diffraction Procedures for Polycrystalline and Amorphous Materials* (Wiley, New York, ed. 2, 1974).
22. We thank G. E. Brown, M. E. Fischer, B. K. Godwal, E. Knittle, H. E. Lorenzana, and Q. Williams for helpful discussions. This work was supported by the University of California Institute of Geophysics and Planetary Physics (Los Alamos National Laboratory), the National Science Foundation, and Exxon Research and Engineering Company. A.M.S. was supported by the Sloan Foundation and the Dreyfus Foundation.

4 October 1991; accepted 23 November 1991

Modeling 100,000-Year Climate Fluctuations in Pre-Pleistocene Time Series

THOMAS J. CROWLEY, KWANG-YUL KIM, JOHN G. MENGEL, DAVID A. SHORT

A number of pre-Pleistocene climate records exhibit significant fluctuations at the 100,000-year (100-ky) eccentricity period, before the time of such fluctuations in global ice volume. The origin of these fluctuations has been obscure. Results reported here from a modeling study suggest that such a response can occur over low-latitude land areas involved in monsoon fluctuations. The twice yearly passage of the sun across the equator and the seasonal timing of perihelion interact to increase both 100-ky and 400-ky power in the modeled temperature field. The magnitude of the temperature response is sufficiently large to leave an imprint on the geologic record, and simulated fluctuations resemble those found in records of Triassic lake levels.

SINCE THE PUBLICATION OF THE HISTORIC Hays, Imbrie, and Shackleton paper in 1976 (*1*), a great deal of attention has been given to the origin of the dominant 100-ky orbital eccentricity signal in late Pleistocene time series of ice volume. Additional studies (*2*) demonstrated that 100-ky fluctuations also occur in other late Pleistocene climate series. Although most modeling studies have linked the 100-ky ice volume fluctuations to nonlinear interactions between the climate system and ice sheets (*3*), a puzzling dilemma arises from examination of climate time series from periods earlier than the late Pleistocene. Records from the Pliocene and early Pleistocene (~1.0 to 2.4 Ma, million years ago), Miocene (~15 Ma), Cretaceous (~100 Ma), and Triassic (~200 Ma) also indicate that 100-ky and sometimes 400-ky climate fluctuations were occurring, but either there is little evidence for the presence of extensive ice sheets during these times or the ice sheets were fluctuating at other dominant periods (*4*). Astronomical times series (*5*) indicate that the most important term in the series expansion for eccentricity is at 413 ky. Furthermore, many of the proxy records are from tropical regions,

T. J. Crowley and K.-Y. Kim, Applied Research Corporation, 305 Arguello Drive, College Station, TX 77840.
J. G. Mengel, Applied Research Corporation, 8201 Corporate Drive, Landover, MD 20785.
D. A. Short, Laboratory for Atmospheres, Code 913, National Aeronautics and Space Administration, Goddard Space Flight Center, Greenbelt, MD 20771.

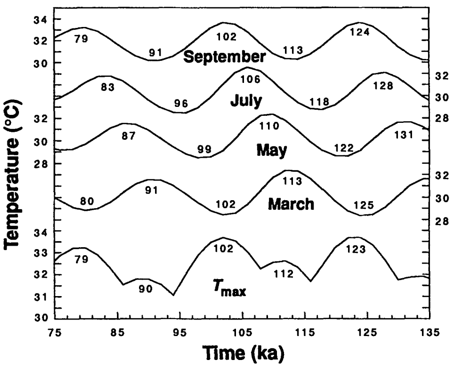

Fig. 1. Modeled time series (0°N, 20°E) for present geography for interval 75,000 to 135,000 years ago. This interval contains three well-known peaks in the ice volume record (*13*). The T_{max} time series represents a composite of a primary autumnal equinox signal and a secondary vernal equinox signal.

that is, they are far removed from influence by any undiscovered pre-Pleistocene ice sheets.

In this paper we propose an explanation for at least some of the tropical 100-ky and 400-ky changes that involves variations in the response of the monsoon system on equatorial land areas subject to twice yearly peaks in solar forcing. We extend an earlier study that examined how the present land-sea distribution filters orbital forcing in the frequency domain (*6*). Both studies utilized a seasonal, two-dimensional energy balance climate model (EBM) that does a reasonable job of resolving the present seasonal cycle (*7*). A number of tests have demonstrated that the model has a sensitivity to seasonal changes in forcing comparable to atmospheric general circulation models [GCMs (*8*)]. Because the EBM is very efficient, it can be used to generate long time series of the seasonal temperature response to orbital insolation changes, something that could not be done with a GCM.

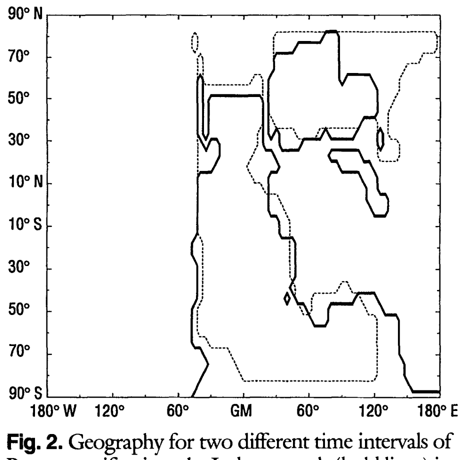

Fig. 2. Geography for two different time intervals of Pangaea unification, the Induan epoch (bold lines) in the Triassic (~225 Ma) and the Pliensbachian epoch (dotted lines) in the Jurassic (~195 Ma). These time periods straddle the interval of lake level deposition (*4*) that is the target test for our model. Geographies are from (*10*).

The earlier study (*6*) showed that a 100-ky response in yearly maximum temperature (T_{max}) is amplified in equatorial land areas as a result of the twice yearly passage of the sun across the equator. In mid- and high-latitude regions, the timing of T_{max} consistently occurs in mid-to-late summer. However, in equatorial land areas, the model shows substantially more variance in the seasonal timing of this index. For example, Fig. 1 illustrates the relation between modeled seasonal temperatures at the equator (Africa) and predicted T_{max} for a well-studied interval—the last interglacial period. This interval includes three sea level highs and is bracketed by glaciations at approximately 70,000 and 135,000 years ago. Eccentricity values are relatively high (0.04 to 0.05) for this time interval, so there are also three well-defined insolation peaks related to the precession cycle.

The effect of the three insolation peaks on T_{max} varies by season (Fig. 1). The T_{max} diagnostic generally tracks the September time series (second of the two overhead passages of the sun). However, there is one major difference between the T_{max} and September records. Whereas the September temperature record displays a typical eccentricity-modulated precession cycle that shows no significant 100-ky power, the T_{max} time series is "clipped," that is, it contains a second set of peaks of lower temperature as a result of the presence of weaker warming peaks in the vernal equinox time series 10,000 years later. Thus, T_{max} can be reached near either the vernal or the autumnal equinoxes, depending on orbital configurations. These variations should represent changes in monsoon forcing, which are significantly affected by precession variations (*9*).

Two reasons justify use of a temperature index that characterizes more than one season. First, in a region such as the equator, the net climate effect of monsoon variations, either locally or far-field, may require assessment of the total changes that occur over the spring-autumn half-year. The T_{max} index takes a step in that direction. Second, geologic records (for example, dust in deep-sea cores) sometimes represent an integrated signal that, in equatorial regions, might well originate from more than one season. For these reasons, we believe T_{max} can be used as a proxy index of monsoon activity.

Long time series (800 ky) of the T_{max} response on the equator (*6*) indicate that the clipping, or the presence of the second peak in the time series, results in a rectified response that transforms power to the modulating frequency. For the Pleistocene, the magnitude of the temperature amplification was only marginally large enough to yield a significant climatic response. However, because the amplification is a function of land-sea distribution (*6*), we postulated that considerably greater amplification would occur on larger landmasses, for example, Pangaea. To test this hypothesis, we generated an 800-ky time series of maximum summer tem-

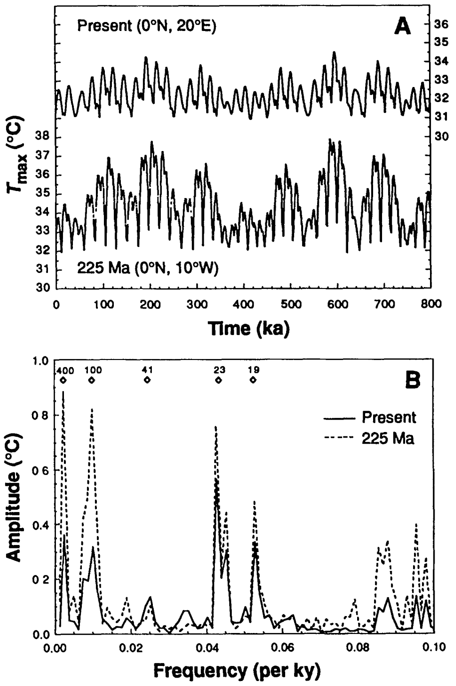

Fig. 3. Comparison of modeled time series for the present and late Triassic. The former record is from (*6*). (**A**) Time domain; (**B**) frequency domain.

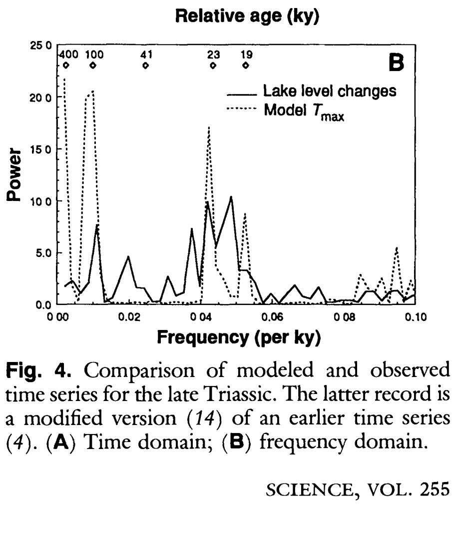

Fig. 4. Comparison of modeled and observed time series for the late Triassic. The latter record is a modified version (*14*) of an earlier time series (*4*). (**A**) Time domain; (**B**) frequency domain.

peratures at the equator on Pangaea, at the time when Triassic lake deposits from eastern North America record 100-ky fluctuations. In order to isolate the effects of geography, we used the orbital forcing of the last 800 ky (*5*) for all runs. Geographic reconstructions (*10*) were available for two time intervals (Fig. 2) bracketing the deposition of the lake sediments, and we illustrate results for the earlier time interval. Because there were relatively small changes in equatorial geography over the interval examined, model-generated time series for both intervals are almost identical. Paleogeography is therefore not a major uncertainty in our simulations.

Because of the presence of the large Pangaean landmass in the Mesozoic, the T_{max} response was substantially greater then than in the Pleistocene (Fig. 3). In addition to higher frequency cycles, a nearly 2.5°C peak-to-peak change in amplitude at 100-ky intervals is evident in the 225-Ma time series. Such fluctuations, especially in the core of the Intertropical Convergence Zone (ITCZ), may well be large enough to leave a significant imprint on the geologic record (*9*). Comparison of the spectra of the two model time series (Fig. 3B) demonstrates the greater power at 100 ky on the Pangaean landmass. Because numerous meteorological investigations have also demonstrated that fluctuations in tropical rainfall also affect climate in higher latitudes, the temperature fluctuations we simulate may well be manifested in other phenomena that we cannot examine with the EBM.

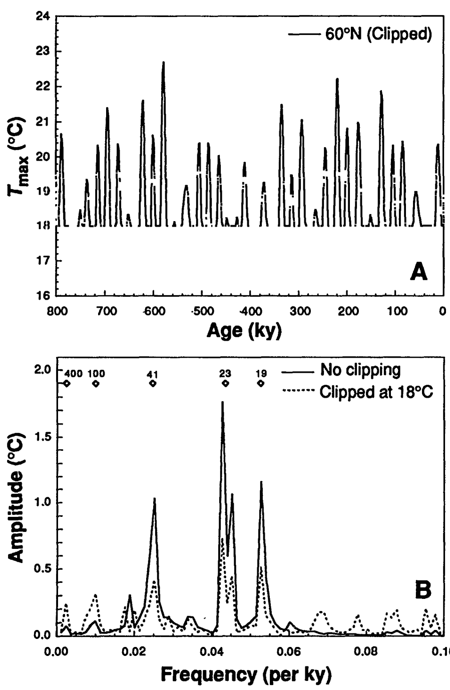

Fig. 5. Assessment of the potential effects of a nonlinear recording system on relative amounts of 100-ky and 23-ky power. The original time series (*6*) represents the T_{max} response to orbital forcing at 60°N, 100°E (central Eurasia). This series typifies a standard eccentricity-modulated precession cycle that has no significant power at 100 ky (*6*). In the "clipped" time series (**A**) all original values <18°C were reset to 18°C in order to mimic the effect of, for example, low lake levels. In neither this case nor others (not shown) were we able to generate 100-ky power in excess of 23-ky power in the time series (**B**).

The predicted time series for equatorial Pangaea is similar to those observed for records from Triassic lakes at 5°N, 10°W (Fig. 4A) (*4*). A spectral comparison (Fig. 4B) indicates that both records have similar statistical properties. One difference is that the 23-ky peak is larger than the 100-ky peak in the observations, whereas the latter is the case in the model. However, because other time series from the same area (*4*) show more power at 100 ky than at 23 ky, it is not clear whether this discrepancy is a major cause of concern.

One potential problem with interpretation of 100-ky power in the Triassic lake series is that our analysis suggests that "clipping" the time series on the cold end will increase 100-ky or 400-ky power in any time series. Such clipping could conceivably reflect nonlinearities in the recording system rather than nonlinearities in the climate system. For example, although lakes may well record relative levels in high stands, during times of increased net evaporation they may not record relative levels of low stands. A lake cannot get any lower than empty. Extreme dry periods might not be recorded, and any time series would tend to show the same clipped features that contribute to strengthening of 100-ky or 400-ky power.

To test the above possibility, we conducted sensitivity tests on a model time series for 60°N, 100°E for present geography (central Eurasia). This record shows a strong eccentricity-modulated precession cycle and no significant 100-ky power (*6*). Artificial clipping of the time series at various levels both reduced power in the precession band and enhanced power at 100 ky and 400 ky (Fig. 5). In none of our clipping experiments were we able to produce 100-ky cycles with more variance than at 23 ky—a pattern evident in some geologic time series. However, because other sedimentary processes may also generate substantial 100-ky power (*11*), this topic warrants more study.

Our hypothesis requires more testing before it can be accepted (for example, with atmospheric GCMs that have explicit moisture cycles). As modeled herein, we only generate significant 100-ky responses on large landmasses in low latitudes. However, monsoon-induced changes in atmospheric circulation could cause changes in high latitudes. They could also affect upwelling or weathering patterns, which might translate terrestrial changes to the marine realm. It may be that 100-ky and 400-ky cycles in the tropics are also affected by other phenomena (for example, variations in the carbon cycle). Diurnal variations in forcing at 100-ky periods (*12*) may also be important for understanding the evolution of the monsoon system.

We initially discovered enhanced 100-ky and 400-ky power in our Quaternary time series as a result of investigations of the filtering effect of geography on Milankovitch insolation cycles. That was a serendipitous discovery, which involved no a priori tuning of the model to conform to preconceived notions of how the system should respond. Even if subsequent studies modify our conclusions, the results emphasize the importance of full seasonal-cycle runs in the study of paleomonsoon systems (most earlier studies have considered only January and July responses). Whether such equatorial variations might also influence late Pleistocene 100-ky ice volume fluctuations requires further investigation.

REFERENCES AND NOTES

1. J. D. Hays, J. Imbrie, N. J. Shackleton, *Science* **194**, 1121 (1976).
2. A. Berger, J. Imbrie, J. Hays, G. Kukla, B. Saltzman, *Milankovitch and Climate* (Reidel, Dordrecht, Netherlands, 1984).
3. G. E. Birchfield, J. Weertmann, A. T. Lunde, *Quat. Res.* **15**, 126 (1981); D. Pollard, *Nature* **296**, 334 (1982); H. LeTreut, J. Portes, J. Jouzel, M. Ghil, *J. Geophys. Res.* **93**, 9365 (1988); B. Saltzman, *Climate Dynam.* **1**, 77 (1987); W. T. Hyde and W. R. Peltier, *J. Atmos. Sci.* **44**, 1351 (1987).
4. M. Briskin and J. Harrell, *Mar. Geol.* **36**, 1 (1980); T. C. Moore, N. G. Pisias, D. A. Dunn, *ibid.* **46**, 217 (1982); N. J. Shackleton, *Progr. Oceanogr.* **11**, 199 (1982); T. D. Herbert and A. G. Fischer, *Nature* **321**, 739 (1986); P. E. Olsen, *Science* **234**, 842 (1986); J. Park and T. D. Herbert, *J. Geophys. Res.* **92**, 14027 (1987); J. Bloemendal and P. deMenocal, *Nature* **341**, 897 (1989); L. A. Mayer, *ibid.* **352**, 148 (1991); G. C. Bond, M. A. Kominz, J. Beavan, in *Sedimentary Modeling: Computer Simulations and Methods for Improved Parameter Definition* (Kansas Geological Survey, Lawrence, in press).
5. A. L. Berger, *Quat. Res.* **9**, 139 (1978).
6. D. A. Short, J. G. Mengel, T. J. Crowley, W. T. Hyde, G. R. North, *ibid.* **35**, 157 (1991).
7. G. R. North, J. G. Mengel, D. A. Short, *J. Geophys. Res.* **88**, 6576 (1983).
8. T. J. Crowley, D. A. Short, J. G. Mengel, G. R. North, *Science* **231**, 579 (1986); W. T. Hyde, T. J. Crowley, K.-Y. Kim, G. R. North, *J. Clim.* **2**, 864 (1989); T. J. Crowley, S. K. Baum, W. T. Hyde, *J. Geophys. Res.* **96**, 9217 (1991); G. R. North, K.-J. Yipp, S.-Y. Leung, R. M. Chervin, *J. Clim.*, in press.
9. COHMAP Members, *Science* **241**, 1043 (1988).
10. J. T. Parrish, A. M. Ziegler, C. R. Scotese, *Palaeogeogr. Palaeoclimatol. Palaeoecol.* **40**, 67 (1982).
11. P. Schiffelbein and L. Dorman, *J. Geophys. Res.* **91**, 3821 (1986); M. Ripepe and A. Fischer, in *Sedimentary Modeling: Computer Simulations and Methods for Improved Parameter Definition* (Kansas Geological Survey, Lawrence, in press).
12. R. S. Cerveny, *J. Geophys. Res.* **96**, 17209 (1991).
13. K. J. Mesolella, R. K. Matthews, W. S. Broecker, D. L. Thurber, *J. Geol.* 77, 250 (1969); A. L. Bloom, W. S. Broecker, J. M. A. Chappell, R. K. Matthews, K. J. Mesolella, *Quat. Res.* **4**, 185 (1974).
14. M. A. Kominz and G. C. Bond, *Earth Planet. Sci. Lett.* **98**, 233 (1990).

15. Supported by NSF grant ATM91-02808 to T.J.C.

7 August 1991; accepted 5 November 1991